

THE ARCHES CLUSTER MASS FUNCTION

SUNGSOO S. KIM,¹ DONALD F. FIGER,² ROLF P. KUDRITZKI,³ AND F. NAJARRO⁴*Accepted for publication in Astrophysical Journal Letters*

ABSTRACT

We have analyzed H and K_s -band images of the Arches cluster obtained using the NIRC2 instrument on Keck with the laser guide star adaptive optics (LGS AO) system. With the help of the LGS AO system, we were able to obtain the deepest ever photometry for this cluster and its neighborhood, and derive the background-subtracted present-day mass function (PDMF) down to $1.3 M_\odot$ for the $5''$ – $9''$ annulus of the cluster. We find that the previously reported turnover at $6 M_\odot$ is simply due to a local bump in the mass function (MF), and that the MF continues to increase down to our 50 % completeness limit ($1.3 M_\odot$) with a power-law exponent of $\Gamma = -0.91$ for the mass range of $1.3 < M/M_\odot < 50$. Our numerical calculations for the evolution of the Arches cluster show that the Γ values for our annulus increase by 0.1–0.2 during the lifetime of the cluster, and thus suggest that the Arches cluster initially had Γ of $-1.0 \sim -1.1$, which is only slightly shallower than the Salpeter value.

Subject headings: Galaxy: center — open clusters and stellar associations: general — stars: luminosity function, mass function — celestial mechanics, stellar dynamics

1. INTRODUCTION

The stellar initial mass function (IMF) is the most primary product of the star formation process. With this one relation, it is possible to directly probe the crucial predictions of star formation models. Surprisingly, the IMF is approximately universal, following the Salpeter law (Salpeter 1995) for masses between 1 and $120 M_\odot$ (Kroupa 2002). On the low mass end, there appears to be a universal rollover around $0.8 M_\odot$, and the high mass end seems to be truncated by a sharp cutoff near $150 M_\odot$ (Weidner & Kroupa 2004; Figer 2005).

However, star formation theories predict that the lower mass cutoff (m_l) should be a function of environmental parameters, i.e. magnetic field strength and cloud temperature (e.g., Bonnell, Larson, & Zinnecker 2006). In the extreme environment of the Galactic center (GC), some of these models predict an elevated lower mass cutoff/rollover with respect to that observed in the disk (Morris 1993). If this prediction is true, then the GC should have an abnormally bright lower mass cutoff, something that has not been *directly* observed anywhere in the Universe.

The best places to trace the IMF near the GC are the two young star clusters therein: the Arches and Quintuplet clusters (see Figer et al. 1999 for findings and early studies on these clusters). These clusters are very young (2–4 Myr), compact ($\lesssim 1$ pc), and only 20–30 parsecs away from the GC in projection, while they appear to be as massive as the smallest Galactic globular clusters ($\sim 2 \times 10^4 M_\odot$; Kim et al. 2000). Of the two clusters, the Arches is preferred for studies of the low-end mass

function (MF) as the Quintuplet is significantly more dispersed.

While the Arches cluster's compactness makes its stars easily identifiable for their high spatial density projected onto the background population, this same property makes confusion a problem at faint magnitudes. Note for scale that a $1 M_\odot$ dwarf has $K \simeq 21$ in the cluster. For instance, the luminosity function (LF) obtained from *Hubble Space Telescope* (HST) NICMOS observations by Figer et al. (1999) for the whole cluster was 50 % complete at $6 M_\odot$. The adaptive optics (AO) science demonstration data observed with the Gemini/Hokupa'a system were analyzed by Yang et al. (2002) and Stolte et al. (2002), who obtained a 50 % completeness level at $5.6 M_\odot$ and a 75 % completeness level at $6 M_\odot$ for the whole cluster, respectively. Stolte et al. (2005) have analyzed the natural guide star (NGS) AO observations of the cluster with the Very Large Telescope NAOS/CONICA system, and derived the MF of the intermediate region of the cluster ($5''$ – $10''$) down to $2.3 M_\odot$ at a 50 % completeness limit.

Although the last study reached the faintest magnitude to date, due to the lack of suitable NGS candidates for neighboring fields, it lacks the observations of nearby background populations, which should be subtracted from the LF/MF of the cluster field to obtain the true cluster LF/MF. It had no choice but to compare the MF from the central and intermediate regions of the cluster ($r < 10''$) with that from the outer region ($r > 13.4''$) to infer the MF of the cluster only. However, while there are almost no bright cluster stars in this outer region, a non-negligible number of faint cluster stars may be present there due to mass segregation. For example, the comparison between HST observations and N -body simulations by Kim et al. (2000) indicates that the tidal radius of the Arches cluster is $25''$ – $30''$. Thus a reliable estimation of the LF/MF of the nearby background populations would require observations of control fields that are at least $30''$ away from the cluster center.

For this reason, we have carried out Keck/NIRC2 laser

¹ Dept. of Astronomy & Space Science, Kyung Hee University, Kyungki-do 446-701, Korea; sungsoo.kim@khu.ac.kr

² Chester F. Carlson Center for Imaging Science, Rochester Institute of Technology, 54 Lomb Memorial Drive, Rochester, NY 14623-5604

³ Institute for Astronomy, University of Hawaii, 2680 Woodlawn Drive, Honolulu, HI 96822

⁴ Instituto de Estructura de la Materia, Consejo Superior de Investigaciones Científicas, Calle Serrano 121, 28006 Madrid, Spain

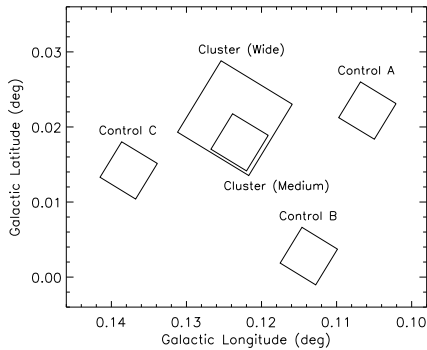


FIG. 1.— Locations of our images in the galactic coordinates. The control fields, which were taken to estimate the stellar density of the nearby background population, are separated $\sim 60''$ from the cluster center.

guide star (LGS) AO observations of the Arches cluster and its nearby background populations to take advantage of the LGS AO system that does not have the distance limit from NGS candidates. Here, we present the analysis of these observations along with results from several relevant N -body simulations.

2. OBSERVATIONS AND DATA REDUCTION

The images were obtained using the Keck/NIRC2 LGS AO system on 2006 May 4 & 5. The Arches cluster ($\alpha = 17^{\text{h}}45^{\text{m}}50^{\text{s}}.59$, $\delta = -28^{\circ}49'20''.3$; J2000) was observed with the medium ($20'' \times 20''$, $0''.0198 \text{ pixel}^{-1}$) and wide ($40'' \times 40''$, $0''.0397 \text{ pixel}^{-1}$) field cameras, and three nearby control fields, separated $\sim 60''$ from the cluster center, were imaged with the medium field camera in order to sample the background population. The locations of these fields in galactic coordinates are shown in Figure 1. All fields were imaged in H and K_s bands in a 9-point dither pattern with a leg size of $2''$. The multiple correlated double sampling (MCDS) mode was used with 10 coadds and a 10 s integration time per coadd, giving a total exposure time of 900 s per field. Obtained Strehl ratios for the K_s (H) images are 0.17 (0.08), 0.19 (0.08), 0.25 (0.06), 0.13 (0.06), and 0.12 (0.06) for the medium cluster field, control fields A, B, C, and wide cluster field, respectively, resulting in FWHMs of 70–100 mas for K_s , and 61–98 mas for H .

For data reduction, the dithered images were first combined by maximizing the cross-correlation. Star finding, point-spread function (PSF) building, and PSF fitting procedures were performed using the DAOPHOT package within the Image Reduction and Analysis Facility (IRAF). The medium field camera PSFs were moderately elongated toward the center of the image due to a relatively small isoplanatic patch obtained during the observations, thus we have allowed the PSFs to be quadratically variable along both axes of the field.

Typical DAOPHOT magnitude errors were less than 0.05 mag down to $K_s \simeq 19$ for stars in the cluster field with $r > 5''$ ($K_s \simeq 18$ for the wide field camera) and $K_s \simeq 19.5$ for stars in the nearby fields. We do not include stars with errors greater than 0.2 mag ($K_s \gtrsim 21.5$) in our analyses. The elongation of the PSF of the medium camera was significant at the four corners of the images, so we excluded stars farther than $10''$ from the image center.

Photometric calibration was done against the

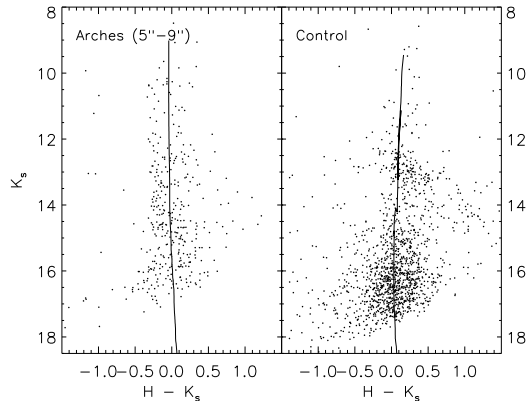


FIG. 2.— Dereddened color-magnitude diagram of the stars with DAOPHOT magnitude errors less than 0.2 mag in the $5''$ – $9''$ annulus of the cluster field (left) and in control fields A, B, and C. Also shown are the solar-metallicity isochrones for 2 Myr (left) and 1 Gyr (right) from the Geneva set of models. The limiting magnitude in H is ~ 1 mag brighter than K_s , so the number of stars shown in the left panel is much smaller than that used for deriving our mass function later, which is based on the K_s -band photometry only.

HST/NICMOS photometry by Figer et al. (1999) assuming that H and K_s magnitudes are identical to NICMOS F160W and F205W magnitudes for the stars in our fields (Kim et al. 2005 and Stolte et al. 2002 indicate that the transformation from H and K' to F160W and F205W filters has a very weak dependence on color for the stars in the Arches cluster).

Completeness tests were performed for all images by adding artificial stars to the observed images with the PSF obtained from our reduction. 800 artificial stars were used per magnitude bin (a total of 7200 stars), but only 200 stars were added per test image. For our analyses in the following sections, we will only consider magnitude and mass bins with a completeness fraction larger than 50 %. Due to the relatively irregular shape of the AO PSFs, the DAOPHOT star-finding algorithm resulted in many bogus stars around bright stars, and we have excluded from our photometry the faint stars that are ~ 4 mag fainter than a nearby (within $\sim 0.55''$ for the medium field camera and $\sim 0.8''$ for the wide field camera), brighter star. Since the central region of the cluster is dominated by bright stars, we will analyze the LF/MF of the intermediate region ($5''$ – $9''$) where the photometry of the faint stars is limited by the background confusion. But there are still a few bright stars in the intermediate region that can hamper the recovery of nearby fainter stars. Since we are more interested in the incompleteness of faint stars by background confusion than that by nearby bright stars, we exclude artificial stars that are ~ 4 mag fainter and within $\sim 0.55''$ ($\sim 0.8''$ for the wide field) from a nearby star from calculating the completeness fractions.

3. RESULTS

3.1. Extinction

For our analyses, we adopt the extinction law by Rieke, Rieke, & Paul (1989; $A_H = 1.56A_K$) and the distance modulus for the GC of 14.52 mag (8 kpc). Stolte et al. (2002) reported color variation of stars as a function of the distance from the cluster center and interpreted it as a local depletion of dust (and thus a smaller extinction)

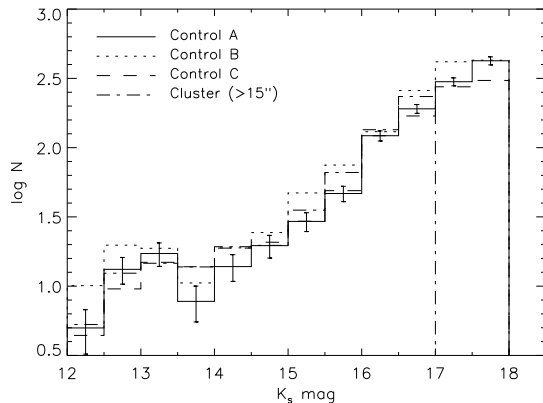


FIG. 3.— Dereddened, completeness corrected K_s -band luminosity function for control fields A, B, and C, and the outer region ($r > 15''$) of the cluster field from the wide field camera, scaled to the area of $5''$ – $9''$ annulus. The histograms are shown only for magnitude bins whose recovery fraction is more than 50 %. Also shown are the Poisson error bars for the control field A.

at the cluster center due to winds from massive stars or photo-evaporation of dust grains by the intense UV radiation field. Our data confirm such variation, and we determine the extinction values for the $5''$ – $9''$ annulus of the cluster field, the outer ($r > 15''$) region of the cluster field, and three control fields separately. Then we assume that stars in the same field or annulus have the same extinction value.

We compare the 2 Myr, solar-metallicity isochrone from the Geneva set of models (Lejeune & Schaerer 2001) to our color-magnitude ($H - K_s$ vs. K_s) diagram (Fig. 2) and obtain an average extinction at K_s of 3.1 ± 0.19 mag for the $5''$ – $9''$ annulus of the cluster field, which is consistent with the extinction value estimated by Stolte et al. (2005) for the same region.

Our control fields and outer region of the cluster field are expected to be composed of stars with a variety of ages and metallicities (Figer et al. 2004). However, $H - K_s$ colors of the stars with intrinsic K_s magnitudes of 1–3 mag, which have underreddened, apparent K_s magnitudes of 18–20 mag at the GC, vary only little ($\lesssim 0.05$ mag; see Kim et al. 2005, for example) for various ages and metallicities. So we compare the 1 Gyr, solar-metallicity isochrone to the $H - K_s$ color distribution of stars with underreddened, apparent K_s of 18–20 mag, and find that our control fields A, B, & C have A_{K_s} of 2.9 ± 0.22 , 3.1 ± 0.17 , & 2.5 ± 0.25 mag, respectively, and the outer region of the cluster field has $A_{K_s} = 3.0 \pm 0.25$ mag (quoted uncertainties are the averages of the extinction spread). Since the amounts of extinction spread are similar in our cluster and control fields, the differential extinction in each field will not cause a problem to our subtraction of background population from the cluster field.

3.2. Background Population

Figure 3 compares the dereddened, completeness-corrected K_s -band LFs for the control fields and that for the outer region ($r > 15''$) of the cluster field obtained with the wide field camera. While the LFs of control fields A and C are quite similar, control field B and the outer region of the cluster field generally have higher LFs than the former. This is probably because the con-

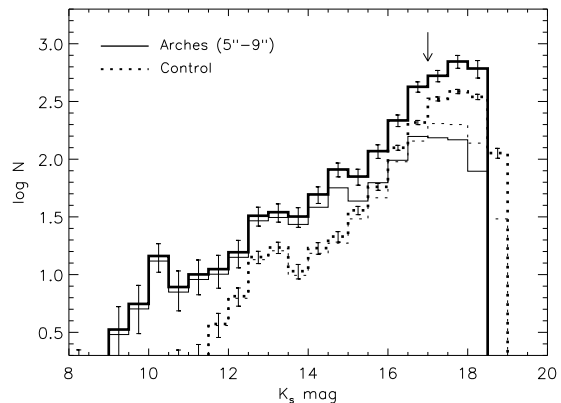


FIG. 4.— Dereddened K_s -band luminosity functions for the $5''$ – $9''$ annulus of the cluster field (*solid*) and the average of the control fields A, B, and C (*dotted*) scaled for the area of $5''$ – $9''$ annulus. *Thin lines* are for the raw LFs and *thick lines* are for the completeness-corrected LFs. The Poisson error bars are shown for the latter. The arrow indicates the 50 % completeness limit for the $5''$ – $9''$ annulus of the cluster field.

trol field B is located closer to the Galactic plane where the stellar density is larger and a part of the outskirts and tidal tail of the Arches cluster might be included in our outer cluster field. We take an average of control fields A, B, and C as the LF of the background population of the cluster. Note that this will probably overestimate the background population toward the Arches cluster slightly since we do not have a control field that is located at the opposite side of the control field B, and thus our estimate for the cluster LF/MF would be a lower limit.

Figure 4 compares the dereddened K_s -band LFs for the background population (an average of control fields A, B, and C) and that for the intermediate region of the cluster field obtained with the medium field camera. The figure shows both raw and completeness-corrected LFs, and the latter of the cluster field is clearly larger than that of the background population at least down to $K_s = 17$ mag, which is the 50 % completeness limit for the cluster field. The H -band LFs give a similar result except that their 50 % completeness limit is 0.5–1 mag brighter than for the K_s band (the limit in H itself is 1 mag brighter than that in K_s , but the typical apparent $H - K_s$ colors of faint stars in the cluster field are 1.5–2 mag).

3.3. The Mass Function

We convert the apparent magnitudes into masses using the Geneva models. Here, we only use K_s -band data as they provide deeper photometry. Figure 5 shows our completeness-corrected MF for the cluster intermediate region after background subtraction, along with the MF from Stolte et al. (2005) that is also completeness-corrected, but *not* background-subtracted; both are scaled to an area of $5''$ – $9''$ annulus. The MF of Stolte et al. (2005) shows a global turnover below $\log M/M_\odot \simeq 0.35$ ($M \simeq 2.3 M_\odot$), which is also their 50 % completeness limit, but our cluster MF, whose 50 % completeness limit is at $\log M/M_\odot = 0.1$ ($M \simeq 1.3 M_\odot$), still has a significant amount of stars below $M = 2.3 M_\odot$ and keeps increasing at least down to $M = 1 M_\odot$. Note that our MF increases even below our 50 % completeness limit.

Stolte et al. (2005) claim that there may be a turnover

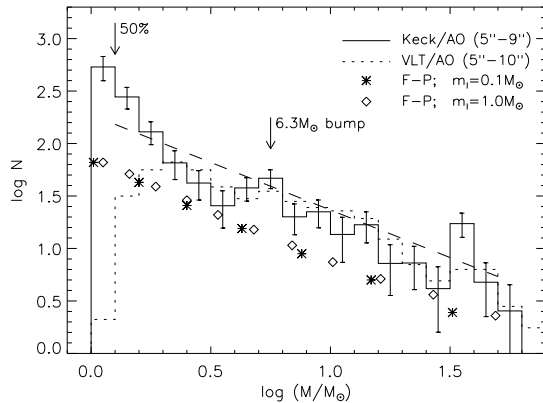


FIG. 5.— Background-subtracted mass functions derived from our K_s -band luminosity function for the 5''–9'' annulus of the cluster field (*solid*) and the mass function of Stolte et al. (2005) for the 5''–10'' annulus of the cluster (*dotted*). Error bars and the best-fit power-law relation ($\Gamma = -0.91$) for $\log M/M_\odot = 0.1$ –1.7 are shown for the former. The average of control fields A, B, and C were used as the background for the former, while the background population was not subtracted for the latter. Also plotted are the MFs for the same projected annulus from our Fokker-Planck calculations that fit the observed MF at 2 Myr the best (offset by -0.5 dex for clear presentation). The *asterisks* are for the calculation with $m_l = 0.1 M_\odot$ and the *diamonds* are for $m_l = 1 M_\odot$. Both calculations have an initial Γ of -1.1 , and total mass of $4 \times 10^4 M_\odot$. The arrows indicate the locations of the 50 % completeness limit and the $6.3 M_\odot$ bump.

near $\log M/M_\odot \simeq 0.8$ ($M \simeq 6.3 M_\odot$) in their MF and that this might indicate a global decrease of the background-subtracted MF below that mass. However, our data, which have a quarter dex lower completeness limit in mass, indicate that the MF globally increases down to our completeness limit even after background subtraction. Therefore, we presume that the turnover around $M = 6.3 M_\odot$ claimed by Stolte et al. (2005) is in fact a local bump in the MF as see in Figure 5. Eisenhauer et al. (1998) find a similar bump in their LF of the Galactic starburst template NGC 3603, and show that such a bump is an indication of the young age ($\lesssim 3$ Myr) using the evolutionary pre-main-sequence tracks by Palla & Stahler (1993).

When fit to a single power-law relation, our cluster MF gives a power-law exponent of $\Gamma = -0.91 \pm 0.08$ (the Sapeiter slope is $\Gamma = -1.35$) for the mass range of $\log M/M_\odot = 0.1$ –1.7. This is slightly steeper than the exponent for massive stars only ($\log M/M_\odot = 0.7$ –1.7), $\Gamma = -0.71 \pm 0.15$.

⁵ These calculations consider internal dynamics of the cluster such as mass segregation and tidal evaporation among others; see

We have performed several Fokker-Planck calculations (for $m_l = 0.1$ & $1 M_\odot$) and N -body simulations (for $m_l = 1 M_\odot$) targeted for the Arches cluster with initial cluster conditions similar to those used in Kim, Morris, & Lee (1999) and Kim et al. (2000), one of which is no initial mass segregation. We find that the Γ values for the projected annulus of 5''–9'' increase by 0.1–0.2 during the lifetime of the Arches cluster, 2–2.5 Myr.⁵ Therefore, our results suggest that the IMF of the cluster has $\Gamma = -1.0 \sim -1.1$. Figure 5 shows two MFs for our annulus from our Fokker-Planck calculations that best match the observed MF at 2 Myr. These two calculations have considerably different m_l 's (0.1 & $1 M_\odot$), but result in nearly identical MFs for the annulus. Thus our estimate for the IMF from the simulations does not sensitively depend on the choice of m_l .

Using the red clump stars in the region $|l| \lesssim 2^\circ$ and $0^\circ.5 \lesssim |b| \lesssim 1^\circ$ that were observed with the Infrared Survey Facility telescope, Nishiyama et al. (2006) newly estimated the near-infrared extinction law toward the inner Galactic bulge. When assuming this extinction law, which is derived by averaging for rather larger region of the GC, is applicable to the stars in our images, we find that the 50 % completeness limit moves down to $1 M_\odot$, but there is almost no change in Γ for our annulus (-0.90 ± 0.09).

Data presented herein were obtained at the W. M. Keck Observatory, which is operated as a scientific partnership among the California Institute of Technology, the University of California, and the National Aeronautics and Space Administration. The Observatory was made possible by the generous financial support of the W. M. Keck Foundation. We appreciate the anonymous referee for valuable comments, which greatly improved our manuscript. S.S.K. thanks Myung Gyoong Lee, Mark Morris, Hong Soo Park, and Andrea Stolte for helpful discussion. This work was supported by the Astrophysical Research Center for the Structure and Evolution of the Cosmos (ARCSEC) of Korea Science and Engineering Foundation through the Science Research Center (SRC) program. The material in this paper is based upon work supported by NASA under award No. NNG05-GC37G, through the Long Term Space Astrophysics program. F.N. acknowledges PNAYA2003-02785-E and AYA2004-08271-C02-02 grants.

the references for model details.

REFERENCES

- Bonnell, I. A., Larson, R. B., & Zinnecker, H. 2006, astro-ph/0603447
 Eisenhauer, F., Quirrenbach, A., Zinnecker, H., & Genzel, R. 1998, ApJ, 498, 278
 Figer, D. F., Kim, S. S., Morris, M., Serabyn, E., Rich, R. M., & McLean, I. S. 1999, ApJ, 525, 750
 Figer, D. F., Rich, R. M., Kim, S. S., Morris, M., & Serabyn, E. 2004, ApJ, 601, 319
 Figer, D. F. 2005, Nature, 434, 192
 Kim, S. S., Morris, M., & Lee, H. M. 1999, ApJ, 525, 228
 Kim, S. S., Figer, D. F., Lee, H. M., & Morris, M. 2000, ApJ, 545, 301
 Kim, S. S., Figer, D. F., Lee, M. G., & Oh, S. 2005, PASP, 117, 445
 Kroupa, P. 2002, Science, 295, 82
 Lejeune, T., & Schaerer, D. 2001, A&A, 366, 538
 Morris, M. 1993, ApJ, 408, 496
 Nishiyama, S., Nagata, T., Kusakabe, N., Matsunaga, N., Naoi, T., Kato, D., Nagashima, C., et al. 2006, ApJ, 638, 839
 Palla, F., & Stahler, S. W. 1993, ApJ, 418, 414
 Rieke, G. H., Rieke, M. J., & Paul, A. E. 1989, ApJ, 336, 752
 Salpeter, E. E. 1955, ApJ, 408, 496
 Stolte, A., Grebel, E. K., Brandner, W., & Figer, D. F. 2002, A&A, 394, 459
 Stolte, A., Brandner, W., Grebel, E. K., Lenzen, R., & Lagrange A.-M. 2005, ApJ, 628, L113
 Weidner, C., & Kroupa, P. 2004, MNRAS, 348, 187
 Yang, Y., Park, H. S., Lee, M. G., & Lee, S.-G. 2002, Jour. of Korean Astron. Soc., 35, 131